Key Engineering Materials
ISSN: 1662-9795, Vol. 926, pp 862-874
doi:10.4028/p-yp2hj3

Submitted: 2021-12-07
Revised: 2022-02-04
Accepted: 2022-02-08
Online: 2022-07-22

Innovative Online Measurement and Modelling Approach for Property-Controlled Flow Forming Processes

Lukas Kersting[1,a,*], Bahman Arian[2,b], Julian Rozo Vasquez[3,c], Ansgar Trächtler[1,4,d], Werner Homberg[2,e] and Frank Walther[3,f]

[1]Fraunhofer Institute for Mechatronic Systems Design (IEM), Paderborn, Germany

[2]Paderborn University, Forming and Machining Technology (LUF), Germany

[3]TU Dortmund University, Chair of Materials Test Engineering (WPT), Germany

[4]Heinz Nixdorf Institute (HNI), Paderborn University, Germany

[a]lukas.kersting@iem.fraunhofer.de; [b]ba@luf.uni-paderborn.de, [c]julian.rozo@tu-dortmund.de;

[d]ansgar.traechtler@iem.fraunhofer.de; [e]wh@luf.uni-paderborn.de; [f]frank.walther@tu-dortmund.de

*corresponding author

Keywords: online sensor application, model for control design, closed-loop control, flow forming

Abstract. The production of complex multi-functional, high-strength parts is becoming increasingly important in the industry. Especially with small batch size, the incremental flow forming processes can be advantageous. The production of parts with complex geometry and locally graded material properties currently depicts a great challenge in the flow forming process. At this point, the usage of closed-loop control for the shape and properties could be a feasible new solution. The overall aim in this project is to establish an intelligent closed-loop control system for the wall thickness as well as the α'-martensite content of AISI 304L-workpieces in a flow forming process. To reach this goal, a novel sensor concept for online measurements of the wall thickness reduction and the martensite content during forming process is proposed. It includes the setup of a modified flow forming machine and the integration of the sensor system in the machine control. Additionally, a simulation model for the flow forming process is presented which describes the forming process with regard to the plastic workpiece deformation, the induced α'-martensite fraction, and the sensor behavior. This model was used for designing a closed-loop process control of the wall thickness reduction that was subsequently realized at the real plant including online measured feedback from the sensor system.

1. Introduction

In industrial appliance, the flow forming process is nowadays performed on specialized CNC-controlled machines [1, 2]. Here the flow forming machines use an integrated closed-loop actuator control with a measured feedback of the actuator's force or position to ensure the actuator motion. In this case, the toolpath is planned offline before forming. This concept disregards the actual workpiece behavior during manufacturing [3]. Since the workpieces are measured offline outside the forming process, deviations between the desired and the resulting workpiece are detected late. This leads in the worst case to reject parts. The challenge is to predict forming effects like springback, to counter unpredicted process disturbances and to ensure the resulting workpiece properties. A promising approach to overcome this challenge is to establish a *closed-loop property control*. The term 'properties' primarily means in this context material and component properties like hardness, residual stresses, surface roughness or micromagnetic behavior and texture [4]. It is also related to geometric properties [3]. This closed-loop control could enhance the complexity of possible workpiece geometries and enables the integration of additional functionality in forming parts. An example for the new functionality is to produce tamper-proof parts with an invisible, magnetic barcode as a unique identifier which could be realized by a locally graded microstructure profile.

Metastable austenitic stainless steels like AISI 304L are appropriate to produce these special parts. These steels generally possess an austenitic microstructure which is non-ferromagnetic. By plastic

deformation, a strain-induced phase transformation from paramagnetic austenite to ferromagnetic α'-martensite can occur [5, 6]. Therefore, the magnetic properties of a workpiece could be selectively adjusted through process parameter modification by a closed-loop property control.

To establish a closed-loop property control into a flow forming process, a real time feedback of the product properties is required. Thus, appropriate sensors for online measurements are necessary to realize this feedback. This paper presents a sensor concept for the online measurement of the wall thickness reduction and the α'-martensite content of the metastable austenitic steel AISI 304L on a modified flow forming machine. In this context, the machine and sensor setup, the machine control architecture and the closed-loop control system are shown. The control system includes a closed-loop wall thickness control and uses online measurements from the installed sensor system. Subsequently, a simulation model of flow forming process is proposed including plastic deformation, austenite-martensite transformation and a sensor model. This model is used for a proof-of-concept of the closed-loop control. Finally, quantitative and qualitative results of the experiments with the above-mentioned closed-loop control are presented for validating the sensor concept using the example of wall thickness reduction.

2. Setup Modules

Flow forming process. The process of flow forming is used for the manufacturing of rotationally symmetric products by plastically deforming a hollow shaft (e.g. tube) with typically a number of co-rotating rollers, which can be performed in consecutive stages or in a single stage [7]. In the process, a hollow shaft is fastened to a mandrel and formed by a moving roller tool adjustable in X- and Y-axis. This leads to a characteristic reduction of the wall thickness. Due to the intended wall thickness reduction, flow-forming can be distinguished from conventional spinning [1]. Two main variations of flow forming are forward- and reverse (or backward) flow forming. The reverse flow forming process used for the investigations is defined by the opposite direction of the rollers feed and the material flow [7].

Specimens. For the experiment, seamless tubes of metastable austenitic stainless steel AISI 304L (X2CrNi18-9, 1.4307) were used as semi-finished products. The tubes have an initial outer diameter of 80 mm and a wall thickness w of 4 mm, with slight variations in terms of wall thickness between maximum value w_1 and minimum value w_2 due to the eccentricity of seamless tubes shown in Fig. 1. The length L of the semi-finished tubes amounts 120 mm.

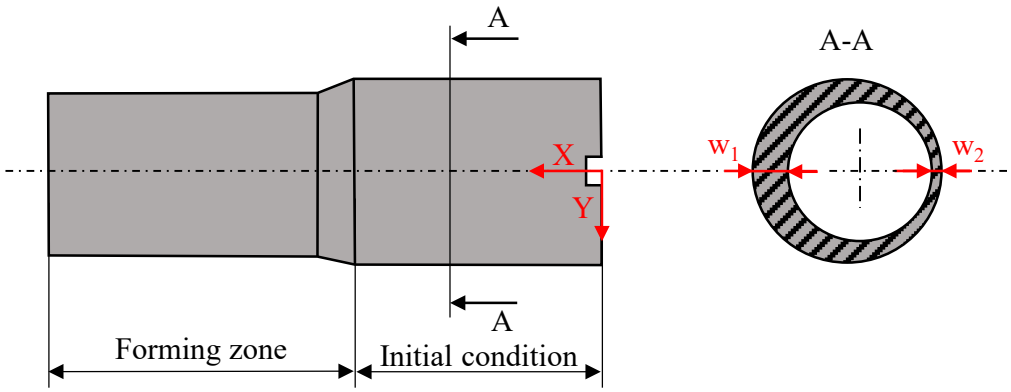

Figure 1. Eccentricity of tubes (maximum initial wall thickness w_1, minimum initial wall thickness w_2)

Machine setup. For the tests, a PLB 400 spinning machine from Leifeld Metal Spinning GmbH (Ahlen, Germany) was used. The machine has a drive power of 11 kW at a maximum achievable spindle speed of 950 rpm. The cross support with its two machining axes is hydraulically driven and was developed at LUF at Paderborn University. Depending on the application, the cross support can be rotated by 90° and can therefore be used for flow forming or friction spinning process, for example.

The support axes of the machine (X/Y-axis) can generate a maximum force of 35 kN. The operating pressure of the external hydraulic unit is 80 bar by default and can be increased up to 120 bar if required. In addition, the support has a universal tool holder for the attachment of tools or tool systems. Fig. 2 shows the machine setup.

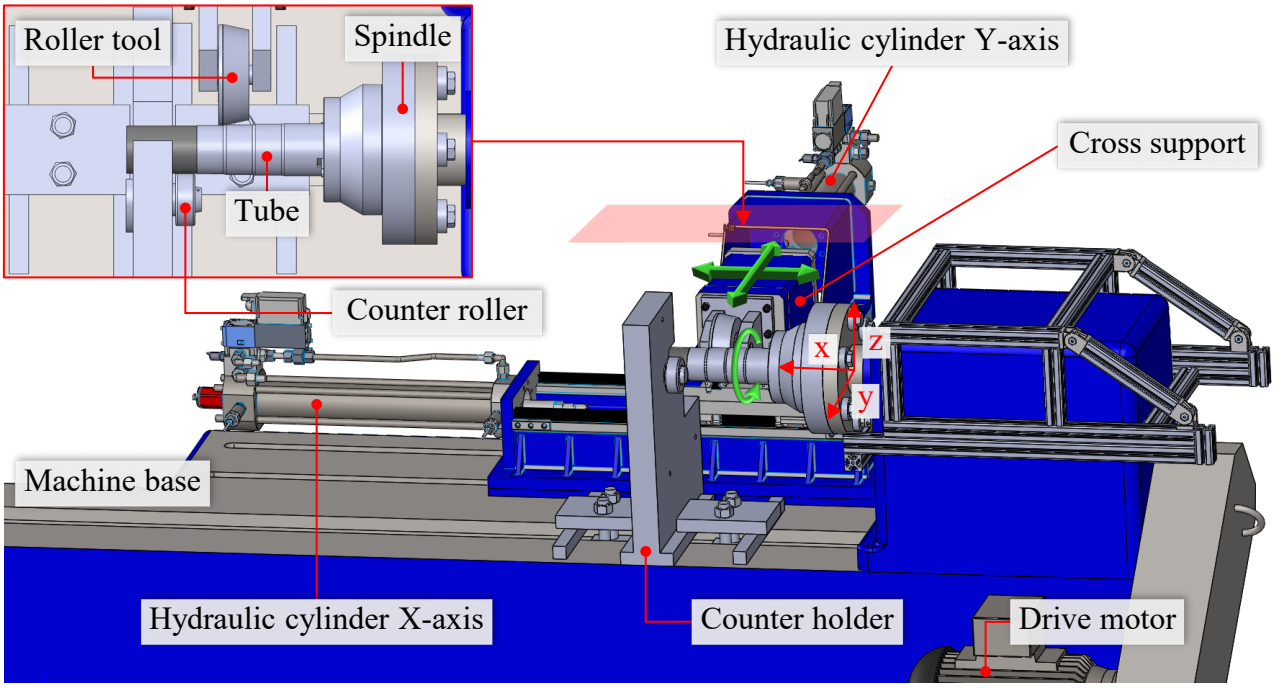

Figure 2. PLB 400 spinning machine (flow forming configuration)

For the investigations, a single-roller tool configuration was used to provide enough space for the sensor equipment applied. The roller has an attack angle of $\alpha = 12°$, a transition radius of $R = 2$ mm and an exit angle of $\beta = 5°$. For the external dimensions, a rolling diameter of 155 mm and a roller width of 46.5 mm can be measured. In the process, a solid counter holder with a ball-bearing counter roller is used to support the mandrel.

Sensor concept. For the integration in closed-loop control for product properties (geometry and α'-martensite content), the Leifeld machine has been equipped with a custom-tailored framework for sensor positioning and alignment developed at LUF. The framework of the sensor system is a construction made of Item-profiles, which is equipped with holders for the sensors to be used. Four identical laser distance sensors are employed and arranged in pairs. Two of those (laser distance sensors 1 and 2) are positioned with axial offset to each other, while pointing perpendicularly at the workpieces surface and measuring along a common axial line. One of the two measuring points is located right in front of the main forming zone and the other one behind or in the forming zone (see Fig. 3). Both measuring points move axially along with the roller tool. The difference in the signals yields the actual wall thickness reduction. Additionally, two stationary laser distance sensors (3 and 4) measure perpendicularly to the tip of the mandrels surface, to detect undesired procedural deflection of the mandrel. These two sensors, arranged orthogonally with respect on each other, allow the localization of the middle axis of the mandrel and therefore of the workpiece.

In addition to geometrical monitoring of the workpiece, the α'-martensite content must also be measured online for closed-loop control of the material properties. For that reason, the micromagnetic 3MA-II sensor is applied close to the forming zone and initially positioned of approx. 1 mm from the workpieces surface for contactless measurement. 3MA-II also moves axially along with the roller tool, thus enabling measurement in the immediate vicinity of the forming zone. Fig. 3 shows the machine setup with the custom-tailored Item-profile framework for the sensors as well as the sensors applied.

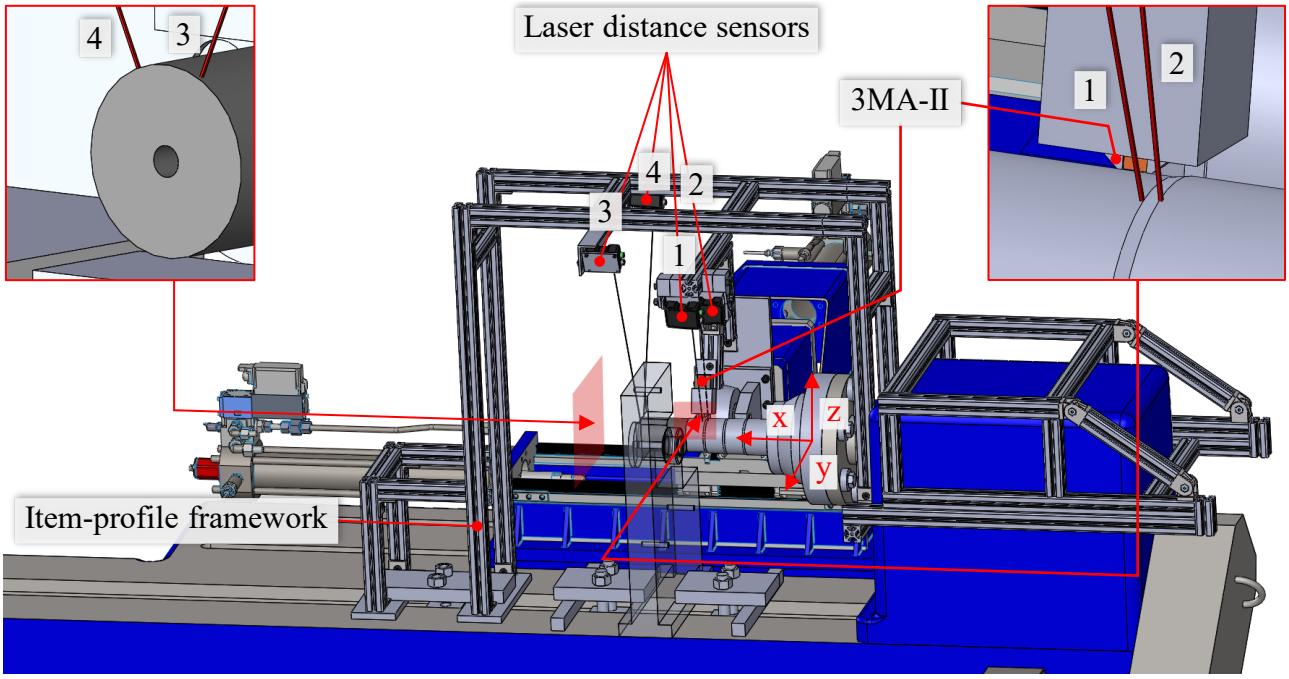

Figure 3. Applied sensor concept at PLB400 spinning machine, including laser distance sensors 1-4 (geometry measurement) and micromagnetic 3MA-II sensor (Barkhausen noise/α'-martensite measurement)

For distance measurement, the laser distance sensor OM70 by Baumer Electric are utilized. The sensors operate using the laser triangulation method. This measuring principle was chosen for closed-loop control because it enables contact-less measurement in large distances of 100 to 600 mm. This is important for safety reason to avoid collisions with the machine support. The sensor has a nominal resolution between 3 and 24 µm. Under real conditions at the forming machine, the measurement quality is negatively affected by interfering light and the curved specimen/mandrel surface. Nevertheless, a resolution of approx. 25 µm is observed in initial tests. Another reason of the optical measuring principle is that the measurement is independent from magnetic fields. Thus, an influence between distance measurement and the micromagnetic 3MA-II is excluded. The micromagnetic measurement as part of the sensor concept is performed by 3MA-II system from Fraunhofer IZFP. The contact-less measurement is used due to the rotating mandrel during forming. For closed-loop control of metastable austenitic steel, Barkhausen noise will be used because in previous investigations a clear correlation between Barkhausen parameter M_{max} and α'-martensite content has been detected [8, 9].

Machine control architecture. The above-mentioned flow forming machine includes an integrated sensor system, a machine control, a host-PC, and the sensor equipment for closed-loop property control (3MA-II and laser distance sensors). The control is programmed in the LabVIEW development environment and executed on a NI compactRIO real-time controller (cRIO 9035). The cRIO is connected via ethernet to the host-PC. The PC has a graphical user interface for programming, operation and monitoring the machine during forming experiment (so-called LabVIEW front panel). The integrated sensor system and the actuators of the machine are directly connected to the cRIO controller. The machine uses hydraulic valves for the machine support. These valves are controlled by an analogue voltage signal. The internal sensor system consists of tool position sensors for a closed-loop actuator position control. These are connected digitally via EtherCAT real time ethernet to the cRIO. The above-mentioned new laser distance sensors for closed-loop property control are also directly connected to the cRIO real-time controller. Therefore, the analogue sensor output and the current measurement module of the cRIO board are used. The sensor outputs the distance as a current signal between 4 and 20 mA. It is reconverted by the control software in a distance value

again. With the experimental setup at the machine, the laser sensor obtains a measuring rate of up to 2 kHz and a response delay of 0.8 ms.

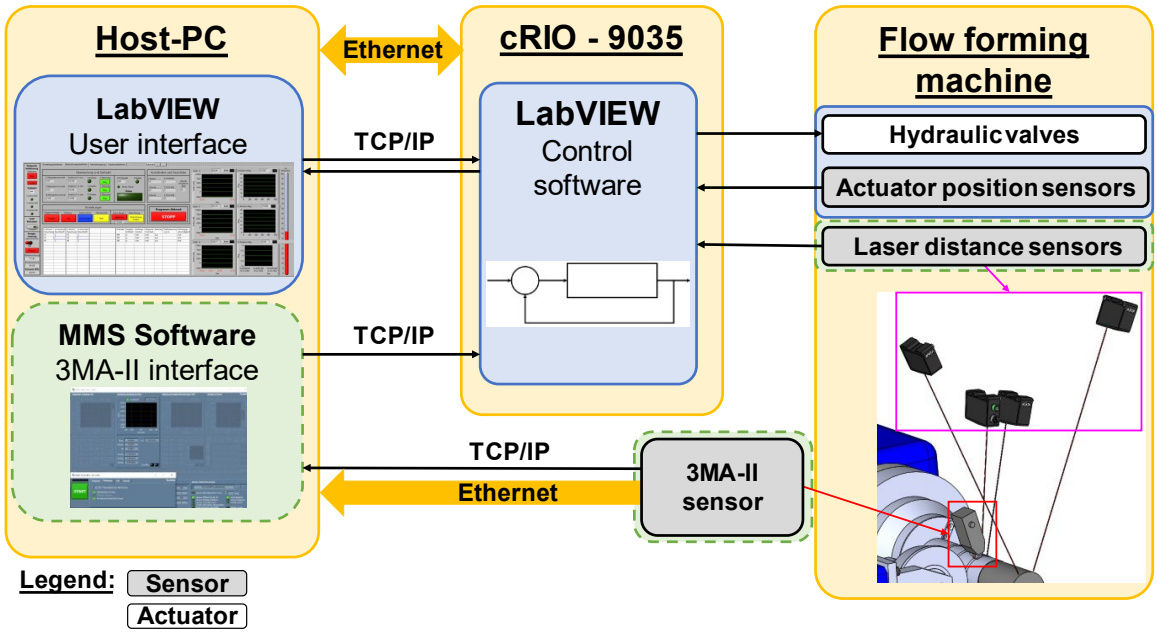

Figure 4. Modified machine control architecture (new components: dashed border, original/modified components: solid border)

The 3MA-II-sensor for property measurement is directly connected via ethernet to the host-PC. On the host-PC, the control software MMS (modular measurement software) is executed to control the 3MA-II-sensor. The communication between the machine control and MMS is established using the TCP/IP protocol. Therefore, the machine control software is supplemented by a TCP/IP client. This special communication structure between sensor and control is chosen because the MMS software is mandatory for measurements with 3MA-II. In preliminary tests, an average data rate of 18 measurements per second was determined with above named setup.

Closed-loop control. The control software includes an integrated closed-loop position and feed control for the machine support in axial and radial direction (see [10, 11]). The control software is extended by an additional closed-loop control for the wall thickness reduction using the laser distance sensors. This control loop is established to ensure the desired workpiece geometry. It is especially relevant due to the single roller tool configuration of the flow forming machine. Here, undesired machine behavior by unbalanced forces (mandrel deflection and bending) and process disturbances effects the resulting wall thickness by forming. In the context of the closed-loop control, wall thickness reduction means the difference of the measurements of the laser distance sensors 1 and 2, one measuring in the forming zone and the other one in the unformed area of the workpiece (see section 2 Fig. 3):

$$\Delta w_{act,mes} = w_{mes,sensor1} - w_{mes,sensor2}. \quad (1)$$

Using only a small gap between the two laser distance sensors, both are nearly identically affected by mandrel deflection, bending and geometrical imperfections like the eccentricity of the tube. Therefore, wall thickness reduction is chosen as an appropriate control variable.

The proposed structure of closed-loop control (Fig. 5) bases on an approach which described in [3]. It includes a (closed-loop) controlled actuator inside an outer control cascade for workpiece measurements, in our case the closed-loop position-controlled roller tool support in radial direction within the outer loop for the wall thickness reduction.

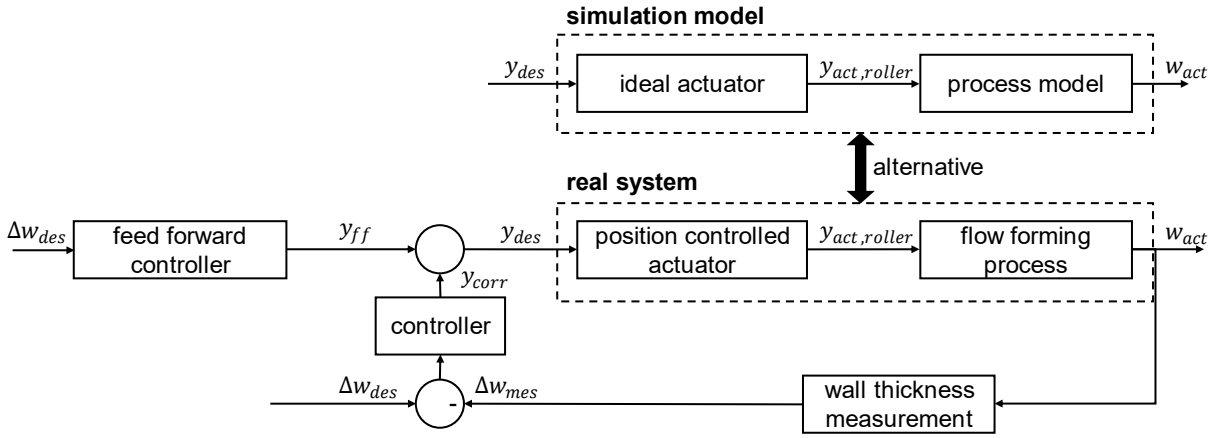

Figure 5. Structure of the closed-loop wall thickness control for use at the real machine and in the simulation model

The proposed structure differs from [3] by using the two-degree-of-freedom structure. Thus, the input signal to the position-controlled actuator of the real system y_{des} depends on the feedback controller (output y_{corr}) and an additional feedforward control (output y_{ff}). The output of the feed forward control y_{ff} is precalculated before forming. In this paper, the infeed needed in the ideal forming process Δr is chosen which is described by:

$$y_{ff} = \Delta w_{des}. \tag{2}$$

The (feedback) controller output y_{corr} is calculated online by the controller comparing the desired wall thickness reduction Δw_{des} to the measured wall thickness reduction in the real process Δw_{mes}. In this paper, a PI-controller is chosen. It is defined as discrete (using trapezoidal integration) due to the implementation in LabVIEW and includes an anti-windup.

It can be stated that the chosen two-degree-of-freedom structure is advantageous because an appropriate roller tool position could be predetermined as nominal state. The feedback controller in this control structure is only used to control deviations from the ideal process – unlike the classical control structure. The feed f in axial direction is not included as control input in this structure. It is defined to be constant during the total forming process. The control structure could also be applied to a martensite closed-loop control using measurements from the micromagnetic 3MA-II-sensor. In that case, the desired martensite content α_{des} would be used instead of Δw_{des} and the actual martensite content α_{mes} would be measured instead of Δw_{mes}.

As shown in Fig. 5, it is possible to substitute the real process in the control structure by a simulation model of the forming process. This feature is used for designing the proposed wall thickness closed-loop control and for virtual testing as a proof of concept before forming at the real machine. As a simulation model, a system model of the forming process is implemented to MATLAB/Simulink. This model is explained in the following section. It enables to simulate the wall thickness reduction for the proposed closed-loop wall thickness reduction control, as well as the martensite content regarding future control approaches.

3. System Model for Control Design

In [12], Riepold et al. already proposed a system model for the forming process of metastable austenitic steels which is based on a geometrical modelling approach by Marini et. al [13]. Riepold et al. use an ideal deformation model and an analytical model of the martensite transformation. In this paper, we extent the approach from [12] by an empiric model for plastic deformation (instead of the ideal deformation) and the sensor system for closed-loop control. For the model, generally an ideal position-controlled actuator is assumed (similar to the control of the real actuator at the forming machine). So the model only contains position-related forming quantities while force-related quanti-

ties like friction are not directly represented. The system model thus distinguishes from alternate modelling approaches for the flow forming process like the time-consuming FEM (e.g. in [14]) and enables simulation durations of less than one minute by contrast. However, the system model will be extended by simulation results from an additional FE model to incorporate force-related effects like friction and residual stresses in future.

Fig. 6 illustrates the base structure of the plant model (without the controller for simplicity). The roller tool position in axial and radial direction ($x_{Roller}(t)$ and $y_{Roller}(t)$) act as input signal to the model (see at the left). The tool position is calculated continuously by the feedback controller and feedforward controller during simulation. The complex system model is modular structured in different subsystems. First, there is an empiric black-box (sub-)model for plastic deformation. Here the resulting wall thickness w and true strain φ_r of the workpiece after forming are calculated in dependance of the workpiece state and the roller tool position. Second, the occurring martensite fraction α' as a result of the plastic deformation and the roller tool feed is determined by an analytical material (sub)model.

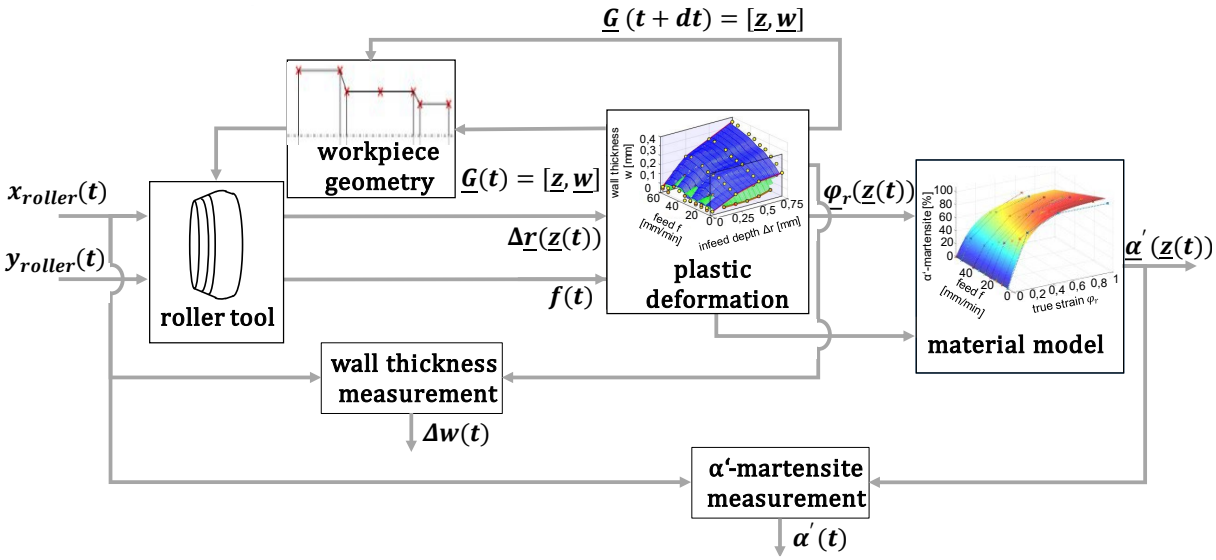

Figure 6. Base structure of simulation model (system model)

Both wall thickness reduction $\Delta w(t)$ and α'-martensite content $\alpha'(t)$ are measured as a time-depending signal by a sensor model representing the sensor system from the real machine (at the bottom of Fig. 6). Including the actuator position as an input and the measured wall thickness reduction as an output, the model is thus suitable to substitute the real process inside the above-mentioned control structure. The various subsystems are explained in more detail in the following sections.

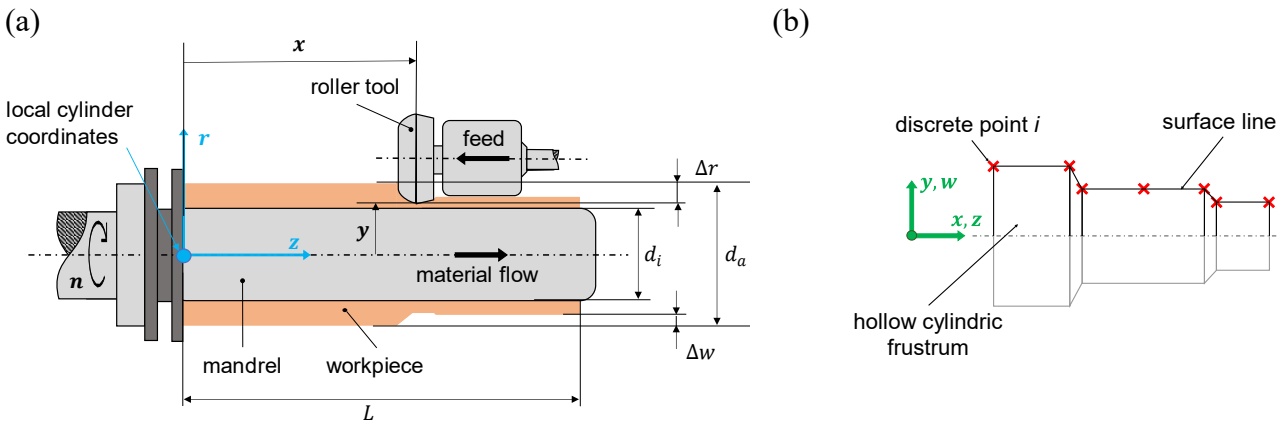

Figure 7. Model of flow forming process: (a) variables (b) discretized workpiece geometry

Workpiece geometry model. In the workpiece geometry model, the forming part geometry is described. For modelling purposes is assumed that the semifinished parts could be described as an axial symmetrical hollow cylinder. Each cylinder has an outer diameter d_a, an inner diameter d_i, a wall thickness $w(t) = 0.5 \cdot (d_a(t) - d_i)$ and the length $L(t)$ (Fig. 7a). By this assumption, the diameters as well as the wall thickness of the semifinished parts are constant in axial and in angular direction. The inner diameter is defined as persistent equal to the mandrel diameter while the outer diameter changes by forming.

In the model, the forming parts are locally discretized in $n-1$ hollow conical frustums, like the approaches in [12] and [13]. Due to the assumed axial symmetry, these parts and frustums are clearly described by its surface line (see Fig. 7b). This line consists of $n-1$ linear line segments which are restricted by n discrete point. Each discrete point $i = 1 \dots n$ is described in the geometry matrix $\underline{G}(t) = \left[\underline{z}, \underline{w}(z)\right](t)$ dim $n \times 2$ by its axial position z and the wall thickness $w(z)$ at z as a measure for its radial position. During the simulation, each z, w in geometry matrix $\underline{G}$ is concurrently actualized by data from the empiric plastic deformation model. The geometry matrix $\underline{G}$ of the workpiece geometry model acts as an input to the roller tool model.

Roller tool model. In the roller tool model, the relation between the roller tool trajectory $u(t) = [x, y](t)$, workpiece geometry $\underline{G}(t) = \left[\underline{z}, \underline{w}(z)\right](t)$ and the process parameters feed f and infeed depth Δr is described. The roller tool trajectory consists of the roller tool positions in axial and radial direction $x(t)$ and $y(t)$ depending on time. Both $x(t)$ and $y(t)$ are specified by the control (see Fig. 6). The axial coordinate $x(t)$ depends on feed $f(t)$ by

$$f(t) = \dot{x}(t) \tag{3}$$

The infeed depth $\Delta r(z(t))$ describes the relation between radial tool position $y(t)$ and the wall thickness $w(z(t))$ before forming (see Fig. 7a). It is determined from the roller tool trajectory $u(t)$ and the workpiece geometry $\underline{G}$ by

$$\Delta r(z(t)) = \begin{cases} (0.5 \cdot [d_i + w(z(t))] - y(t), & d_i + w(z(t)) > y(t) \wedge x(t) < L(t) \\ 0, & otherwise \end{cases}. \tag{4}$$

The case distinction in Eq. 4 considers that forming only occurs where the roller intrudes into the material of the forming part. As a basic simplification of the model, an ideally punctiform roller is assumed. Thus, there is only one single discrete position $z(t)$ and discrete point i where the workpiece is deformed at the same moment. This plastic deformation is calculated by the plastic deformation model where the roller tool model acts as input.

Plastic deformation model. In real forming, the wall thickness reduction distinguishes from the infeed depth because of several effects like elastic springback [15]. According to [15], plastic deformation depends on infeed depth $\Delta r(z(t))$, on feed $f(t)$ and the wall thickness before forming $w(z(t))$. Thus, the occurring wall thickness after forming $w(z(t + dt))$ is modelled by an empiric three-dimensional characteristic curve. The input-output correlation of this black-box model is generally described by

$$w(z(t + dt)) = g(\Delta r(z(t)), \mathrm{w}(z(t)), f(t)). \tag{5}$$

The characteristic curve is parameterized with experimental data presented in [15]. The data contains different feeds $f(t)$ from 0.1 mm/s to 1 mm/s, infeed depths $\Delta r(z(t))$ from 0.5 to 1 mm and wall thicknesses between 1.5 mm and 4.0 mm. Outside this range of f, Δr and w, the experimental data is extrapolated. Including non-ideal forming effects in Eq. 5, the model presented significantly differs from the approach, Riepold et al. presented in [12].

From Eq. 5, the wall thickness reduction is obtained by the difference of the wall thickness before and after forming on the same axial position z:

$$\Delta w(z(t)) = w(z(t+dt)) - w\big(z(t)\big). \tag{6}$$

Finally, the elongation of the part is included to the model based on the calculated wall thickness reduction. The material flow in axial direction is a direct consequence from plastic deformation in radial direction. Here the approach of volume constancy according to [12] and [13] is used. Comparing the volume of the hollow frustrum (described by surface line and the discrete points) before and after forming, the elongation of the volume element (length l_i) is described by

$$\Delta z_i = \int_{z=0}^{l_i} \frac{(2w(z)+d_i)\cdot\Delta w(z)-\Delta w^2(z)}{(d_i+w(z)+\Delta w(z))^2-(0.5d_i)^2}\,dz. \tag{7}$$

This affects all the volume elements and discrete points which are already formed since in backward flow forming the material flow occurs in the opposite direction to the roller movement [12]. In the model, both axial and radial plastic forming effects lead to modified z and w in the geometry matrix. Thus, a new $\underline{G}(t+dt)$ is obtained. The resulting wall thickness w (after forming) from the plastic deformation model is used to calculate the radial true strain as an input to the material model.

Material model. The forming process model incorporates an analytical model of the martensite transformation which is adapted from [12] by Riepold et al. The model generally is based on the sigmoidal Gompertz function and Olson-Cohen model [16] for description of the strain-induced nucleation and growth of α'-martensite in austenitic steels [17]. In [12], the authors have already evidenced, that a sigmoidal model depending on the radial true strain as an input variable is appropriate to describe the martensite fraction in the special flow forming process of austenitic steels. Radial true strain is here defined as

$$\varphi_r = \ln\left(\frac{\Delta w+w}{w}\right). \tag{8}$$

Here Δw possesses a negative sign according to Eq. 6. Thus, φ_r is negative. Besides true strain, in flow forming processes the martensite fraction which results from the forming process also depends on feed [12]. For this reason, the model here presented used the following analytic equation from [12]:

$$\alpha' = \left[A_0 + A_1 \exp\left(-abs\left(\frac{\varphi_r}{A_2}\right)\right)\right][B_0 + B_1 f]. \tag{9}$$

Eq. 9 includes the absolute value due to the sign of φ_r. The equation is parameterized with experimental data presented in [15]. The data results from the same experiments as used for Eq. 5 in this paper. Similar to the workpiece geometry and wall thickness, α' could vary in axial direction of the workpiece. According to Eq. 9, this is due to a change of feed or true strain and wall thickness. For this reason, α' could be specified as a function of the axial position $z(t)$ for each discrete point i. All these different martensite fractions in axial direction are summarized in matrix $\underline{E} = \left[\underline{z}, \underline{\alpha'}\right]$. This matrix $\underline{E}$ and the matrix $\underline{G}$ from the workpiece model act as inputs to the sensor model.

Sensor model. The sensors in the modelled forming process output a time-depend signal from a specific measuring point. Thus, the sensor model is used to evaluate geometry matrix $\underline{G}$ and the martensite matrix $\underline{E}$ at the specific measuring point. It is assumed that the sensors for wall thickness reduction and martensite measurement are mounted on the moving roller tool support. Therefore, the sensor signal in the model is described as a function of the roller tool position $x(t)$ and the geometry or martensite matrix after forming:

$$\Delta w(t) = h\left(x(t), x_{off1}, x_{off2}, \underline{G}(t)\right), \tag{10}$$

$$\alpha'(t) = q\left(x(t), x_{off,mart}, \underline{E}(t)\right). \tag{11}$$

In Eq. 10 and 11, the axial displacement of the sensors relative to the tool position $x(t)$ is considered by the offsets x_{off1}, x_{off2} and $x_{off,mart}$. Thus, the influence of the measuring point to the measured sensor signal is included to the model. Sensor dynamics are considered to be neglectable for simplicity due to the slow process speed. This assumption is confirmed by first measurements from the real plant.

4. Validation of the Sensor Concept

The sensor concept from section 2 is validated by forming experiments using the closed-loop wall thickness control at the real forming machine. The experiments were performed in two steps: simulation and real forming experiment. For each experiment, a single pass with a target wall thickness reduction of Δw_{des} = 0.4 mm was considered and a feed of f = 0.25 mm/s. As the output of the feed forward control, the value 0.4 mm (in simulation) and 1 mm (real plant) were specified. At the first step, the control structure was used for virtual forming experiments to confirm the feasibility of the closed-loop control. It means to proof whether it is possible to control a specific target wall thickness. After the proof of concept by the simulation, the control structure was used at the real forming machine. The final controller parameters were chosen empirically so that the control acts fast but aperiodically.

Results. In Fig. 8a, the simulation result for closed-loop wall thickness control is shown in comparison to open loop control. With open-loop control (dotted line), the wall thickness is reduced to 3.863 mm (reduction of 0.137 mm) using an infeed depth of 0.4 mm. This is caused by the real forming effects, which are implemented in the model by the three-dimensional characteristic curve (section 3). The desired wall thickness reduction of 0.4 mm (to a wall thickness of 3.6 mm) is reached in simulation by the using the closed-loop control (solid line).

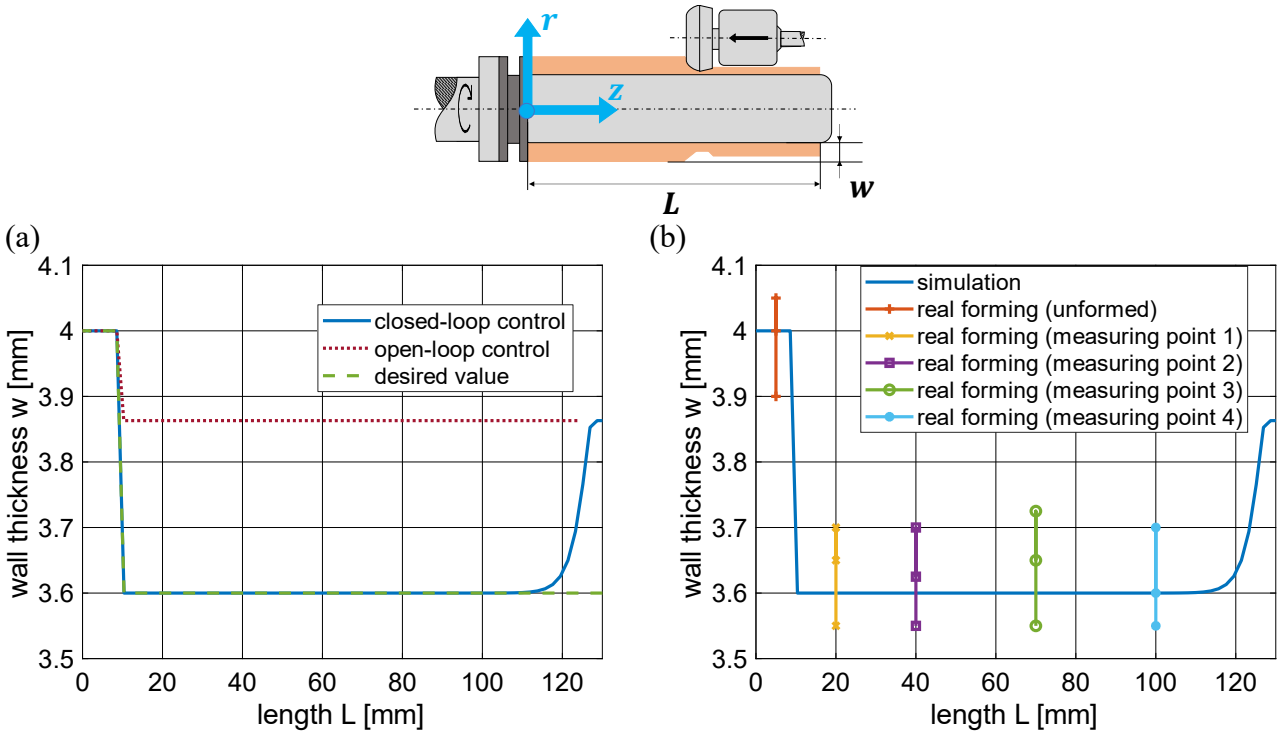

Figure 8. Results of closed-loop wall thickness control experiments: (a) simulation, (b) in comparison with real forming

Between closed-loop and open-loop control both parts differ in length due to the different elongation of the part under different wall thickness reductions that result from volume constancy. A characteristic feature of the simulated geometry is the trough-shaped wall thickness profile. The settling time of the controller with continuous feed in axial direction leads to a curvy shape at the right. This settling length amounts to approx. 20 mm. At the left, the wall thickness rises because the forming zone ends. In the experiments at the forming machine, the same control behavior is determined as in simulation. The parts were additionally measured manually after forming at different measuring points along the part length and in circumferential direction for evaluation. Measurements were performed using the measuring gauge Kroeplin D4R50. As shown in Fig. 8b, with closed-loop control a nearly constant wall thickness in axial direction is reached just like in the simulation. The wall thickness varies at the single measuring points in circumferential direction. This effect was measured in the unformed formed area (at the left of Fig. 8b) as well as in the formed. So, it can be stated that the circumferential deviation is due to the tube eccentricity. It can be summarized: The infeed depth is successfully adjusted by the controller. Thus, the desired wall thickness reduction is reached in simulation and at the real forming plant. The measurement signal from laser distance sensors in the real forming experiment is adequate to be used as feedback for the controller because the experiments with closed-loop control succeed.

During the forming experiments with experimental setup, additional effects were observed:

1. The infeed depth by the controller differs in simulation and in the experiments at the real plant. At the machine, a relatively large infeed depth of 2.25 mm is calculated by the controller for a wall thickness reduction of 0.4 mm. In simulation, only an infeed depth of 0.882 mm is necessary. These differences between simulation und real experiment are probably due a lower machine stiffness than assumed for the model. Despite of the deviation, the same wall thickness (reduction) is reached in simulation as well as in the forming experiments (Fig. 8b). This reveals a decisive advantage of a closed-loop control compared to a precalculated (open-loop) control without sensor feedback: It becomes possible to compensate model deviations online during the process.
2. Distinctive grooves were observed on specimen surface from the real forming experiment. Further experiments without closed-loop control show that these surface grooves and the roughness can be reduced by multiple forming passes. Thus, the usage of multiple passes in the closed-loop control could be a feasible approach that will be investigated soon.
3. Preliminary online measurements with the micromagnetic 3MA-II system were already performed at the flow forming machine. Here the martensite formation was qualitative observed through the increase of the measured Barkhausen noise parameter M_{max}. In the experiments, M_{max} was measured with an accuracy of 0.06 V during forming. A model-based softsensor is under development for the quantitative determination of the α'-martensite fraction from the M_{max} value. In previous work it was already shown that the Barkhausen noise is also affected by the feed (see [12,15]). During the preliminary online measurements, an influence of the distance between sensor and workpiece surface was observed. Thus, the softsensor will also include additional variables to compensate these effects. Additional investigations incl. the usage of the 3MA-II in a closed-loop control and the soft sensor approach are a subject of our current research and will be published soon.

5. Conclusion and Outlook

Closed-loop property control is a promising approach to enhance the flow forming process, to increase the product complexity, functionality and geometric accuracy. An innovative sensor concept for online measurements during the process and its implementation to a modified flow forming machine were presented, including laser distance sensors to measure the wall thickness reduction and a micromagnetic sensor for the martensite content of the part. These measurements are required as a feedback for a closed-loop control. Additionally, a simulation model was presented which contains an empiric model of the plastic deformation during flow forming, an analytic material model of martensite formation and a sensor model. The simulation model is pre-configured to be integrated in

the closed-loop control for the wall thickness reduction as well as the α'-martensite fraction substituting the real forming machine. In this paper, it was used to test the closed-loop wall thickness reduction control as a proof of concept. At the modified flow forming machine, the closed-loop wall thickness control was utilized for forming experiments including the laser distance sensors from the presented sensor concept. By the results, the concept was successfully validated using the example of the laser distance sensors.

In further research, the micromagnetic sensor will also be integrated in a closed-loop control. A model-based softsensor will be used to determine the martensite fraction from the measured Barkhausen noise parameter M_{max}. For the final property control it is planned to concurrent control both – wall thickness reduction and martensite fraction. For this reason, the closed-loop control is to be further developed into a model predictive control (MPC) that includes the simulation model already presented.

Acknowledgements

The authors would like to thank the German Research Foundation (Deutsche Forschungsgemeinschaft, DFG) for their support of the depicted research within the priority program SPP 2183 "Property-controlled metal forming processes", through project no. 424335026 "Property control during spinning of metastable austenites".

References

[1] C.C. Wong, T.A. Dean, J. Lin, A review of spinning, shear forming and flow forming processes, International Journal of Machine Tool & Manufacture 43 (2003) 1419-1435, DOI: 10.1016/S0890-6955(03)00172-X.

[2] M. Runge, Spinning and Flow forming: spinning and flow forming technology, product design, equipment, control systems, Verlag Moderne Industrie, Landsberg/Lech, 1994.

[3] J.A. Polybank, J.M. Allwood, S.R. Duncan, Closed-loop control on product properties in metal forming: A review and prospectus, Journal of Materials Processing Technology 214:11 (2014) 2333-2348, DOI: 10.1016/j.jmatprotec.2014.04.014.

[4] J.M. Allwood, S.R. Duncan, J. Cao, P. Groche, G. Hirt, B. Kinsey, T. Kuboki, M. Liewald, A. Sterzing, A.E. Tekkaya, Closed-loop control for product properties in metal forming, CIRP Annals – Manufacturing Technology 65 (2016) 573-596, DOI: 10.1016/j.cirp.2016.06.002.

[5] J. Talonen, P. Apegren, H. Hänninen, Comparison of different methods for measuring strain induced α-martensite content in austenitic steels, Material Science and Technology 20:12 (2004) 1506-1512, DOI: 10.1179/026708304X4367.

[6] P. Haušild, V. Davydov, J. Drahokoupil, M. Landa, P. Pilvin, Characterization of strain-induced martensitic transformation in a metastable austenitic stainless steel, Materials and Design 31 (2010) 1821-1827, DOI: 10.1016/j.matdes.2009.11.008.

[7] D. Marini, D. Cunningham. P. Xirouchakis, J.R. Corney, Flow forming: A review of research methodologies, prediction models and their applications, International Journal of Mechanical Engineering and Technology 7:5 (2016) 285-315.

[8] M.R.N. Astudillo, M.N. Nicolás, J. Ruzzante, M.P. Gómez, G.C. Ferrari, L.R. Padovese, M.I. Pumarega, Correlation between martensite phase transformation and magnetic Barhausen noise of AISI 304 steel, Procedia Materials Science 9 (2015) 435-443, DOI: 10.1016/j.mspro.2015.05.014.

[9] J. Rozo Vasquez, B. Arian, M. Riepold, W. Homberg, A. Trächtler, F. Walther, Microstructural investigation on phase transformation during flow forming of the metastable austenite AISI 304, in: A. Neidel (Ed.), Fortschritte in der Metallographie, Saarbruecken, 2020, pp. 75–81.

[10] D. Hornjak, Grundlegende Untersuchungen der Prozess- und Werkzeugparameter und ihre Wechselwirkungen für das thermo-mechanisch unterstützte inkrementelle Umformverfahren des Reib-Drückens, Doctoral Dissertation, Paderborn University, Shaker, Aachen, 2013.

[11] B. Lossen, Ein Beitrag zur Herstellung von hybriden Bauteilen mittels Reibdrücken, Doctoral Dissertation, Paderborn University, Shaker, Düren, 2019.

[12] M. Riepold, B. Arian, J. Rozo Vasquez, W. Homberg, F. Walther, A. Trächtler, Model approaches for closed-loop property control for flow forming, Advanced in Industrial and Manufacturing Science 3:100057 (2021), DOI: 10.1016/j.aime.2021.100057.

[13] D. Marini, J. Corney, A methodology for assessing the feasibility of producing components by flow forming, Production & Manufacturing Research 5:1 (2017) 210-234, DOI: 10.1080/21693277.2017.1374888.

[14] M. Houillon, E. Massoni, E. Ramel, 3D FEM Simulation of the Flow Forming Process Using Lagrangian and ALE Methods, AIP Conference Proceedings 908 (2007) 257-262, DOI: 10.1063/1.2740821.

[15] B. Arian, W. Homberg, J. Rozo Vasquez, F. Walther, M. Riepold, A. Trächtler, Forming metastable austenitic stainless steel tubes with axially graded martensite content by flow-forming, ESAFORM 2021 24th International Conference on Material Forming Liège (2021), DOI: 10.25518/esaform21.2759.

[16] G.B. Olson, M. Cohen, Kinetics of strain-induced martensitic nucleation, Metallurgical Transactions A 6 (1975) 791-795, DOI: 10.1007/BF02672301.

[17] M. Smaga, F. Walther, D. Eifler, Deformation-induced martensitic transformation in metastable austenitic steels, Materials Science and Engineering A 483-484 (2008) 394-397, DOI: 10.1016/J.MSEA.2006.09.140.